Cement and Concrete Research 40 (2010) 1488–1494

Contents lists available at ScienceDirect

Cement and Concrete Research

journal homepage: http://ees.elsevier.com/CEMCON/default.asp

The effect of polycations on early cement paste

I. Pochard [a], C. Labbez [a,*], A. Nonat [a], H. Vija [b], B. Jönsson [c]

[a] Laboratoire Interdisciplinaire Carnot de Bourgogne, UMR 5209 CNRS, Universite de Bourgogne, 21078 Dijon Cedex, France
[b] National Institute of Chemical Physics and Biophysics, Akadeemia tee 23, 12618 Tallinn, Estonia
[c] Theoretical Chemistry, Chemical Center, POB 124, S-221 00 Lund, Sweden

ARTICLE INFO

Article history:
Received 11 March 2010
Accepted 1 June 2010

Keywords:
Cement paste (D.)
Polymers (D.)
Tensile properties (C.)
Bridging force

ABSTRACT

This paper studies the possibility for improving the ductility of cement based materials by means of oligocationic additives. Actually, the setting of cement is due to ionic correlation forces between highly negatively charged C–S–H nanoparticles throughout a calcium rich solution. The main drawback of this strong attraction is its very short range that results in low elastic deformation of hydrated cementitious materials. A way to enlarge the attraction range between C–S–H particles would be to add cationic oligomers that would compete with calcium ions modifying the ionic correlation forces via a bridging mechanism of longer range, which could lead to a more ductile material. The studied parameters were the polymerization degree, the separation distance between the charged monomers and the balance between oligocations and monovalent and divalent cations in the solution. The results, both experimental and numerical by Monte Carlo (MC) simulations, demonstrate that cationic oligomers can compete with calcium cations as counterions to the C–S–H surface. The cohesive forces between C–S–H surfaces, calculated by MC simulations, show an interesting behaviour where range and magnitude can be tuned with oligomer concentration, polymerization degree and line charge density. Thus, it seems possible to modulate the ductility and critical strain of cement by addition of cationic oligomers.

1. Introduction

Concrete, i.e. a mix of Portland cement and aggregates, is the most used material in the world for housing and infrastructure construction. In addition to its good compressive strength properties, this omnipresence is explained by the low cost and worldwide availability of cement constituents, which happen to be the main elements of the earth's crust (Si, Ca and O). However, concrete exhibits poor tensile strength, which usually is compensated by the use of iron bars. In this paper, we propose a new route to improve the tensile properties of hydrated cement.

Calcium silicate hydrate (C–S–H) the main hydration product of cement is recognized as responsible for the setting and hardening of cement. While discussed for a long time, the particulate nature of C–S–H is now recognized [2–4,6–9,33]. The size and shape of particles and the structure of aggregates are still a matter of debate [10,11] but experimental observations reveal nanosized platelets [3,12,13,33]. The silanol groups at the surface of C–S–H can titrate and give rise to a high negative surface charge density under high pH and calcium concentration [14]. According to classical colloidal theory [15,16], where the repulsion comes from the electrical double layer interaction, while the attraction is due to van der Waals forces, such charged surfaces should repel each other. At least, increasing the surface charge density of the particles should lead to increased repulsion, which is opposite to what is found in cement paste! AFM experiments [17,18] reveal that C–S–H particles, immersed in a lime ($Ca(OH)_2$) solution, repel each other at low pH while they exhibit a strong attraction at short range (2 nm) provided that pH exceeds 10 ($Ca(OH)_2 > 1$ mM).

Ion–ion correlations are not included in the classical DLVO theory and some years ago [19,20], we demonstrated that the inclusion of these gives rise to a net attractive double layer interaction on purely electrostatic ground. The ion–ion correlations become important in strongly coupled systems, that is high surface charge densities and/or multivalent counterion concentrations, which led Delville and co-workers [21–24] to suggest that this correlation induced attraction is responsible for the setting of early cement paste.

The correlation attraction can be modulated in several ways; decreasing pH of the solution would lead to a weaker attraction as would the replacement of the divalent calcium ions with e.g. monovalent sodium ions. These effects are well-known from cement chemistry and are also reproduced in theoretical calculations [25]. The main drawback of this attraction is its very short range, which results in low elastic deformation of hydrated cementitious materials.

Another way to modulate the interaction between charged colloids is by addition of oppositely charged polyelectrolytes as is done in many technical applications [26–31]. Monte Carlo simulations show that oppositely charged polyelectrolytes can give rise to

* Corresponding author.
E-mail address: christophe.labbez@u-bourgogne.fr (C. Labbez).

0008-8846/$ – see front matter © 2010 Elsevier Ltd. All rights reserved.
doi:10.1016/j.cemconres.2010.06.002

attractive interactions between charged colloids or particles [32] via a bridging mechanism. The bridging attraction from oppositely charged polyelectrolytes is akin to the ion–ion correlation and of comparable magnitude, but it can be made more long ranged. A more long ranged attraction should in principle lead to a more ductile material. The range of the bridging attraction from polyelectrolytes can be varied by: i) the polymerization degree, i.e. the chain length, ii) the charge density of the polymer, i.e. the separation between charged monomers and iii) the balance between polyelectrolytes and monovalent and divalent counterions in the solution.

Based on these observations and with the perspective of obtaining a more ductile final concrete we have made some attempts to incorporate cationic oligoelectrolytes into cement paste. Cationic polyelectrolytes usually acquire their charge from N groups, which titrate and become neutral in basic solution. This can, however, be overcome by quaternizing the N groups. Here we report a combined theoretical and experimental adsorption study of such cationic oligoelectrolytes on C–S–H.

2. Theoretical procedure

2.1. A simple C–S–H model

The structure of the C–S–H particles is not well-known, but it is generally agreed that it is a nanocrystalline material with a lamellar structure close to that of tobermorite [1,5,12,13,33,34]. The dimension of the particles can vary depending on calcium and silicate concentrations, but typical dimensions are of the order of $60 \cdot 30 \cdot 5$ nm^3. Eventually, these platelets grow all around the cement grains and form a gel network that also fills the spaces between grains [35], as schematically drawn in Fig. 1a. Thus, it is a network of C–S–H platelets that binds the composite mass together and the crucial interaction is that between the platelets.

The silanol groups of the surface of C–S–H can titrate and give rise to a negative surface charge density, see Eq. (1) below. Unfortunately, the titration properties of the silicate moieties in C–S–H are not fully characterized. Indeed, in the $CaO–SiO_2–H_2O$ system, the invariant point where silica and C–S–H coexist is situated at pH ~10. This means that C–S–H exists only at pH values above this limit and, as a consequence, C–S–H does not exhibit a point of zero charge and titration experiments can only give a net increase of the surface charge density as a function of pH and ionic strength. Despite these experimental limitations, we have been able to set up an accurate model for the charging process of C–S–H combining simulations and experiments of potentiometric titrations and of electrokinetic in various bulk conditions, see [14] for more details. To be short, in our simulations a C–S–H particle consists in an infinite surface decorated with explicit titratable sites regularly distributed on a square lattice, see Fig. 1b. The site density has been set equal to that of tobermorite, that is 4.8 sites/nm^2. A pK_0 value of 9.8 was assigned to the silanol groups which is equal to that of the first deprotonation reaction of silicic acid.

We do not attempt to model the C–S–H system in atomic detail, but instead we aim at a mesoscopic model that contains basic physical ingredients. Underlying the approach is the assumption that the electrostatic interactions are the most important ones. Hence, we seek a model that incorporates these in an accurate and efficient way. The primitive model of electrolyte solution is such an alternative, where all ions are considered explicitly while water is treated as a dielectric continuum, characterized by its dielectric permittivity, $\epsilon_r = 78.5$ (at room temperature). Besides the charges, the primitive model contains yet another parameter and that is the hard core radius of the ions. This can in some cases be used as a fitting parameter, but in the present simulations we have tried to minimize the influence of the hard core and used the same diameter for all ionic species, $d_{hc} = 4$ Å. The polycation chains are modeled by n charged beads connected by freely jointed rigid bonds. The beads and ions were modeled as charged hard spheres. In an attempt to minimize the number of parameters and maintain a simple model, we have put all ionic diameters, d_{hc}, equal to 4 Å.

2.2. Monte Carlo simulations

The Monte Carlo simulations of the system depicted in Fig. 1b were performed in a grand canonical ensemble. We have used two variants of the model system, where the first, which was used in the majority of simulations, consists of two charged walls that form a slit confining an electrolyte solution in equilibrium with a bulk solution that contains, in addition to ordinary simple ions, also polycation chains (Fig. 2). A second model system containing one neutral wall and another one decorated with titratable sites, as described above, was used to model the experimental adsorption data conducted on dilute dispersions of C–S–H particles. In the second model system the separation, h, between the walls was chosen to be large enough to ensure the existence of a bulk solution inside the simulation box. The sites are allowed to titrate following a grand canonical titration

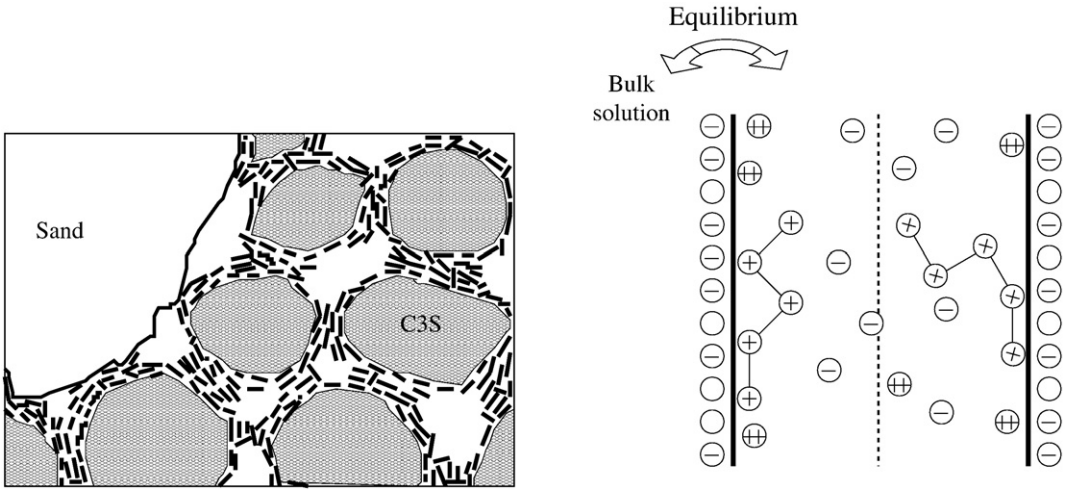

Fig. 1. Left: cartoon of early cement paste, where a small portion of the clinker has gone into solution and formed C–S–H platelets drawn as black bars. Right: a simplified model of two C–S–H platelets with neutralizing divalent counterions (Ca^{2+}) and cationic oligoelectrolytes as well as coions. The platelets are assumed to be infinite in two dimensions and the surface charge density is represented by titrating sites whose charge is determined by pH. The ionic concentrations in the slit are determined by the equilibrium with an infinite bulk solution. The dielectric permittivity, ϵ_r, is assumed to be uniform throughout space and the whole system is electroneutral.

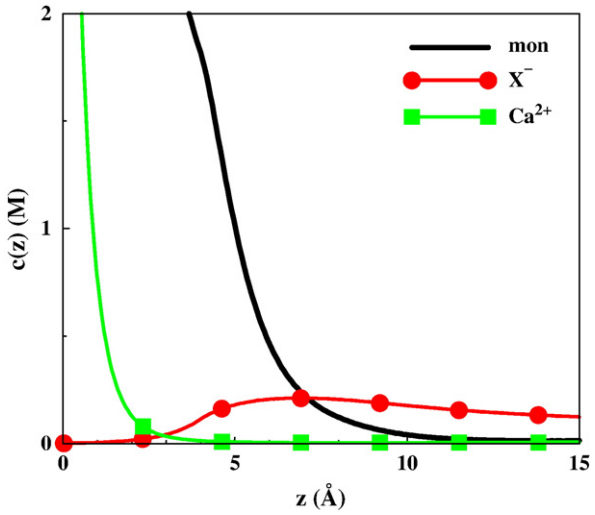

Fig. 2. Example of simulated concentration profiles for the charged species in the slit. Black solid line = monomer, green line with squares = Ca^{2+} and red line with spheres = monovalent coion.

procedure [36], which mimics the protonation and deprotonation of the silanol groups on the C–S–H particles. The procedure has been successfully applied to describe the overcharging of C–S–H by calcium ions [14] and the titration of silica particles [37]. Briefly, the titration process can be described as,

$$\mathrm{SiO{-}H} \rightleftharpoons \mathrm{SiO^-} + \mathrm{H^+} \tag{1}$$

for which the equilibrium constant is defined as,

$$K_0 = \frac{a_{\mathrm{SiO}} a_{\mathrm{H}}}{a_{\mathrm{SiOH}}} \tag{2}$$

where a_i is the activity of species i in Eq. (2). The pK_0 of the silanol groups on the surface of the C–S–H particles is set equal to the one of silicic acid (pK_0 = 9.8). The ionization of a sites corresponds to a change in the charge status, i.e. 0 when protonated and −1 when deprotonated. For the deprotonation, we imagine a two step process: the release of the proton from the surface site, which is followed by the exchange of the ion pair (H^+, B^-; B = base) from the MC box to the bulk. The corresponding Boltzmann factor for the trial energy is

$$\exp(-\beta\Delta U) = \frac{N_B}{V}\exp[-\beta(\mu_B + \Delta U^{el}) + \ln 10(\mathrm{pH}-\mathrm{p}K_0)] \tag{3}$$

where μ and N_B represent the chemical potential and the number of ions B^-, respectively, V is the volume and ΔU^{el} the change in electrostatic energy. An analogous expression holds for protonation. Note that the protons are not treated explicitly, but are accounted for through the constant pH.

The interaction energy between any two ions can be formally described by:

$$u(\mathbf{r}_i, \mathbf{r}_j) = \frac{Z_i Z_j e^2}{4\pi\epsilon_0\epsilon_r |\mathbf{r}_i - \mathbf{r}_j|} \quad r > d_{hc} \tag{4}$$

$$u(\mathbf{r}_i, \mathbf{r}_j) = \infty \quad r < d_{hc} \tag{5}$$

where e and ϵ_0 are the elementary charge and dielectric permittivity for vacuum, respectively. Besides their mutual interactions, the ions also interact with the charged surface sites in the simulation box. Electrostatic interactions are long ranged, and a correction term approximating interactions outside the MC box has been added [38,39].

The osmotic pressure of the confined solution, p_{osm}^{conf}, may be calculated at the mid plane,

$$p_{osm}^{conf} = k_B T \sum_i c_i(mp) + p^{hc} + p^{corr} + p^{bridge} \tag{6}$$

where *mp* stands for mid-plane. The term p^{corr} comes from the fact that ions on either side of the mid-plane correlate and give an attractive contribution to the pressure. p^{bridge} originates from the bridging of the walls by the charged chains of oligoelectrolytes giving an attractive contribution to the pressure. The finite size of the ions gives rise to a repulsive hard core term, p^{hc}. Eq. (6) gives the osmotic pressure in the confined region, but the experimentally interesting quantity is the *net* osmotic pressure,

$$p_{osm}^{net} = p_{osm}^{conf} - p_{osm}^{bulk} \tag{7}$$

where the bulk pressure is calculated for a bulk [40] with the same chemical potential(s) as the double layer.

An ordinary grand canonical procedure [41] is suitable for maintaining chemical equilibrium with simple electrolytes. This is based on a brute deletion and addition to an arbitrary position of the cation and anion of the electrolyte. However, for charged species such as oligomers the probability for a successful insertion of a charged chain as well as its counterions is negligible, and chemical equilibrium is never reached. This can be circumvented by the use of a biased Monte Carlo technique originally introduced by Rosenbluth [42]. The technique has been used for calculating the chemical potential of small polymers [43–46] as well as polyelectrolytes [47]. The polycation chain configurations were sampled by a combination of two MC moves: translation of the whole chain and reptation [48].

Oligocations with various chain lengths were studied with bond lengths of 5 and 10 Å. The oligomer concentration was varied from 1 to 15 mM, while that of simple ions varied between 1 and 20 mM for Ca^{2+} and 100 to 200 mM for Na^+. Typically, the ratio of reptation step to insertion and removal step was adjusted to 80%. The length of the runs varied and a system with high density and long chains requires up to $3 \cdot 10^5$ MC cycles for production after 10^4 cycles of equilibration.

3. Experimental procedure

3.1. Synthesis of quaternized oligoelectrolytes

The pH of ordinary cement paste is high, typically >12.5, and essentially the only possible cationic polyelectrolyte type is a quaternized amine. By using small oligoelectrolytes instead of commercially available polyelectrolytes we avoid problems of polydispersity and facilitate the comparison with simulations. The synthesis started from the commercially available unmethylated substances:

- Diaminopropane; $R_3N^+ - (CH_2)_3 - N^+R_3$
- nor-Spermidine; $R_3N^+ - (CH_2)_3 - N^+R_2 - (CH_2)_3 - N^+R_3$

with $R = H$ and after quaternization $R = CH_3$. Note that when $R = H$ the amine groups are neutral.

3.1.1. Quaternized amine

Permethylated amine was dissolved in acetonitrile and 1.1 equivalents of methyl iodide were added for each amino group. The reaction mixture was heated to 40 °C for 20 h. Diethyl ether was added and the precipitated quaternized amine filtered off and washed with further diethyl ether and dried in vacuum.

3.1.2. Permethylation of diaminopropane

2.2 g (25 mmol) diaminopropane was dissolved in 18 mL formic acid and 15 mL of 37% formaline and the mixture was heated to 110 °C for 20 h. After the reaction mixture had cooled, concentrated KOH was added to increase pH above 12 and the temperature was kept below 25 °C. Permethylated diaminopropane was extracted three times with diethyl ether and dried on Na_2SO_4. The diethyl ether was evaporated and the remaining 3.1 g permethylated diaminopropane was purified through distillation in vacuum (10 mm Hg). A fraction (1.7 g) boiling at 50 °C was collected and finally quaternized as described above.

3.1.3. Permethylation of nor-spermidine

26 g (200 mmol) nor-spermidine was added slowly to 220 mL formic acid. 200 mL 37% formalin was added and the reaction mixture was kept at 110 °C for 24 h. The sample was cooled to 0 °C and 50 mL 3 M H_2SO_4 was added. While stirring 10 g of NaBH4 was added in small quantities and the temperature was kept below 10 °C. The reaction mixture was filtered and extracted with diethyl ether. Concentrated KOH was added in order to increase pH above 12 and the temperature was kept below 20 °C. Permethylated nor-spermidine was extracted three times with diethyl ether and dried on Na_2SO_4. Diethyl ether was evaporated and 15 g product was purified through distillation in vacuum (1 mm Hg) and 6 g of permethylated diaminopropane and 4.5 g of permethylated nor-spermidine were collected at 37 and 87 °C, respectively. The latter was quaternized as above giving a final 19 g of quaternized nor-spermidine. An attempt was also made to quaternize spermine, but the quality of the final product was not satisfactory.

3.2. Adsorption experiments

C–S–H suspensions of 0.9% volume fraction were obtained by mixing analytical grade calcium oxide (Prolabo), colloidal silica TA92 (Rhodia) and distilled-deionized milli-Q water. The obtained dispersion was then aged during three weeks.

3.2.1. Adsorption of oligoelectrolytes on C–S–H

Increasing amounts of oligoelectrolytes were added to various batches of C–S–H suspensions of 30 g each. The mixtures were vigorously shaken during three weeks. After that, the pH of the suspensions were measured with a high alkalinity pH electrode and the electrokinetic measurements were performed by electrophoresis using a Malvern NanoZS apparatus. Afterwards the suspensions were centrifuged at 9000 rpm from which the supernatant solutions were taken. Oligoelectrolyte, calcium and sodium contents in these supernatants were measured by Total Organic Carbone analysis (Shimadzu TOC-5000A) and inductively coupled plasma absorption optical spectroscopy (ICP-OES Vista Pro Varian), respectively. The adsorbed amounts of oligoelectrolytes were then deduced from subtracting the content of oligoelectrolyte remaining in the supernatant from the added amount of oligoelectrolyte in the initial suspensions. The specific surface area of C–S–H is difficult to determine properly. Instead, the adsorbed amount was measured relative to the total amount of Si, which is known from the preparation of the suspensions.

4. Results and discussion

4.1. Forces between C–S–H platelets

From previous studies [23,25] we know that the interaction between two highly charged surfaces like C–S–H is strongly attractive in the presence of divalent calcium ions. It is also well-known both experimentally and theoretically [26,32] that oppositely charged polyelectrolytes can induce an attractive interaction between charged colloids. Fig. 3 confirms these results and also indicates that flexible oligoelectrolytes offers an extra parameter to vary both the width and

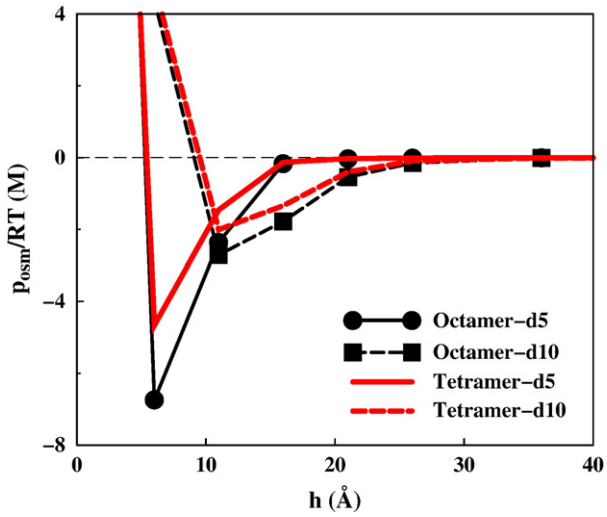

Fig. 3. The osmotic pressure between two titratable surfaces in the presence of cationic oligoelectrolytes at two different bond lengths between monomers, 5 Å(d5) and 10 Å(d10). The surface sites have a $pK_0 = 9.8$ and the monomer concentration in the bulk is 1 mM.

strength of the attraction. A high line charge density gives (or equivalently a short monomer–monomer separation, d = 5 Å) a strong but short ranged attraction, while a less charged polyelectrolyte (d = 10 Å) can give rise to a more long ranged, but weaker attraction.

A crucial aspect is how the oligoelectrolytes can compete with calcium as counterions to the ionized silanol groups on the C–S–H surface and how this affects the interparticle force. This is illustrated in Fig. 4 where the osmotic pressure between two C–S–H surfaces is given for a bulk containing an increasing amount of cationic tetramers and 20 mM of $Ca(OH)_2$. With a low concentration of oligoelectrolyte, calcium will take over and the force will be strong and short ranged characteristic of a calcium dominated system. Increasing the concentration of oligomer swings the competition and the interaction becomes weaker and more long ranged. However, the range of the attraction can become even wider if the oligomer and calcium concentrations are finely tuned.

The C–S–H surface is negatively charged due to the titrating silanol groups and the surface charge density will vary not only with pH but

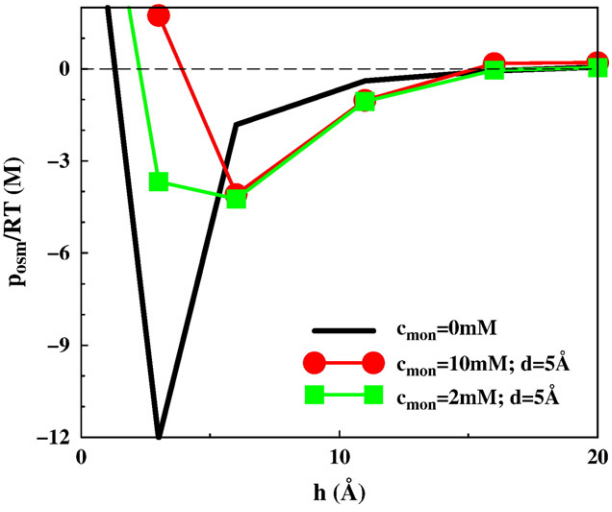

Fig. 4. The osmotic pressure between two titratable surfaces in the presence of both divalent cations and cationic tetramers. The surface sites have a $pK_0 = 9.8$ and the bulk contains various amount of oligoelectrolyte and 20 mM $Ca(OH)_2$.

also with the type of counterion—see Fig. 5. For a given pH there is a considerable change in surface charge density with the valence of the counterion. As one would expect, oligoelectrolytes lead to a stronger negative surface charge density than monovalent sodium ion. Interestingly enough, the titration curve obtained with cationic trimer lies below that with calcium ion, even though trimer carries one extra charge compared to calcium ion. This is explained by the internal entropy of trimers (which is null in the case of calcium). The observed reduced cohesion in a cement paste rich in sodium can be rationalized as a consequence of i) a reduced surface charge density making ion–ion correlations less important and ii) an increased repulsion from replacement of calcium counterions by sodium ions.

Generally, the surface will be neutralized by a mix of calcium ions, cationic oligoelectrolytes and sodium ions. Thus, there will be a competition between the three species—with the characteristic property that the higher the surface charge density the more favoured is the most "highly charged" counterion. In a competition between calcium and sodium, the former will always win. However, as pointed out above, the outcome of a competition between calcium ions and an oligoelectrolyte is less obvious—both the number of charges and their separation in the oligoelectrolyte play important roles.

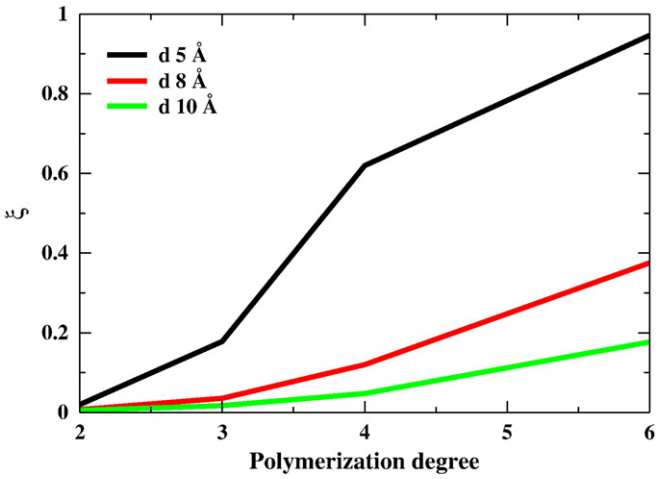

Fig. 6. Simulated adsorbed amount of oligoelectrolyte on a smeared out charged surface, ξ, versus the degree of polymerization for various bond lengths, *d*. The adsorbed amount is given as the ratio of adsorbed monomer and total amount of surface charges. The Ca^{2+} concentration is set to 20 mM throughout the simulations and the charge density is 3 e/nm^2 (0.48 C/m^2).

4.2. Oligomer adsorption on C–S–H

To illustrate how the polymerization degree and bond length between charged monomers as well as the concentration of the different species affect the competition between calcium ions and oligocations we first present some simulation results. Then, a comparison between Monte Carlo simulation results and experimental results of electrophoretic mobility and oligocation adsorption is given.

4.2.1. Simulation results

Fig. 6 shows the dependence of the oligomer adsorption as a function of the polymerization degree for various bond lengths for a wall bearing a smeared out surface charge, set to 3 e/nm^2, in equilibrium with a bulk solution containing 5 mM cationic oligomer and 20 mM $Ca(OH)_2$. This figure clearly illustrates the increased monomer adsorption with both the degree of polymerization and the linear charge density (decrease of the bond length between monomers). The competition between calcium and oligocation for the charged surface is often won by calcium (most of ξ values are below 0.5). In this case, it is only when the linear charge density is high and the polymerization degree is greater than 4 that the oligocations overcome the calcium ions in the double layer.

In Fig. 7 the monomer adsorption on a smeared out surface charge next to a bulk electrolyte solution containing $Ca(OH)_2$ and either cationic dimer or cationic hexamer is plotted for varying oligocation concentration at three different calcium concentrations. As can be seen, the monomer adsorption drops as the bulk calcium concentration is increased. As pointed above, longer chains are more efficient in competing with calcium ions.

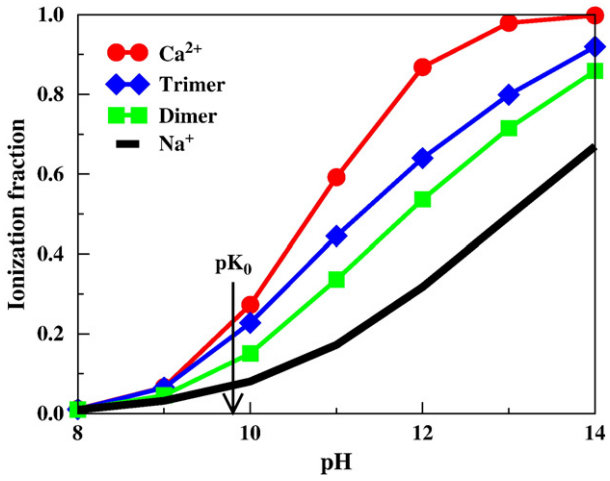

Fig. 5. Simulated titration curves for C–S–H in the presence of Na^+ (black line without symbols), Ca^{2+} (red line with circles), cationic dimer (green line with squares) and trimer (blue line with diamonds). In all cases the bulk salt concentration is 2 mM and the coion is assumed to be monovalent. Bond length between monomers is set to 5 Å.

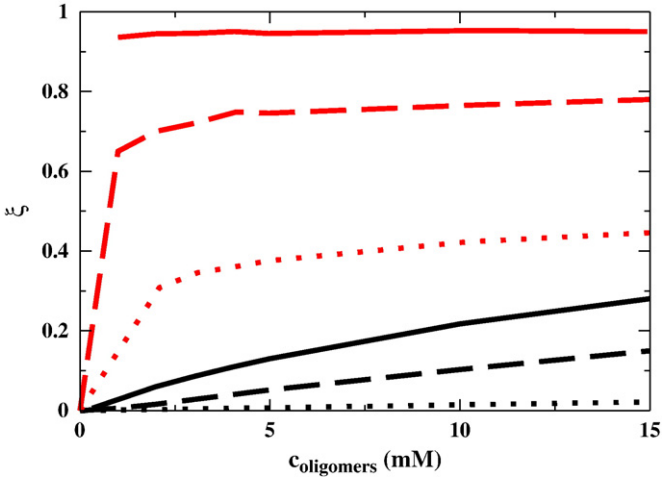

Fig. 7. Simulated adsorbed amount of cationic dimer (black lines) and cationic hexamer (red lines) on a smeared out charged surface, ξ, as a function of their equilibrium bulk concentration at three different calcium concentrations: 20 mM (dotted lines), 5 mM (dashed lines) and 1 mM (full lines). The adsorbed amount is given as the ratio of adsorbed monomer and total amount surface charges. The charge density of the surface is set to 3 e/nm^2 (0.48 C/m^2) and the monomer separation to 8 Å. Note that with hexamers and with a low calcium concentration, the C–S–H particles are predicted to be completely covered with oligomers. Considering a specific surface area of 300 m^2/g the adsorbed mass is, in this case, about 0.34 mg/m^2.

4.2.2. Comparison between experiments and simulations

The adsorption experiments have been performed at high pH (12.5), while the electrokinetic measurements have been done at both high (12.5) and low pH (10).

Fig. 8 shows the adsorption of two oligoelectrolytes on C–S–H at high pH and high calcium content. The number of Si atoms approximately reflects the maximum number of titratable sites and we will use the ratio of adsorbed charges to number of Si atoms, denoted ξ, as a measure of adsorbed amount. From simple electrostatic arguments one would expect the quaternized norspermidine (trimer) to adsorb better than the quaternized diaminopropane (dimer). This is indeed the case as demonstrated in the figure. From the knowledge of the total number of titrated sites (see Fig. 5) and the adsorbed amount of oligomer (Fig. 8) we can conclude that the major part of the silanol groups are neutralized by calcium ions—approximately 90% when the bulk monomer and calcium concentrations are the same. The experimentally determined adsorption is in excellent agreement with the simulation results—the latter are shown as dashed curves in Fig. 8.

4.3. Electrophoretic mobility of C–S–H

The surface charge density of the C–S–H particles is regulated by pH and at pH > 13 essentially all silanol groups are ionized if calcium is the dominating counterion. At a reduced pH, only a fraction (≈0.2) of the silanol groups is ionized as shown in Fig. 5. This means that the competition for the surface between the cationic species becomes weaker and based on the results of Fig. 8 we would then expect the oligoelectrolytes to contribute more, in relative terms, to the neutralization of the surface and to the force.

This is illustrated in Fig. 9 through electrophoretic measurements of C–S–H/oligocation systems at lower pH and calcium content. The expectation, from previous studies [49,50], is that addition of multivalent species should lead to an increase of the electrophoretic mobility and that it will eventually change sign from negative to positive. This is a consequence of an apparent charge reversal [51] of the C–S–H particles [14]. Fig. 9 shows that the addition of oligoelectrolyte leads to an increased mobility. The effect is more pronounced for the trimer as expected and the mobility becomes eventually slightly positive. Fig. 9 also contains simulated potentials for the same cases and these display the same behaviour as the mobilities further strengthening the conclusion that the oligoelectrolytes adsorb on the C–S–H surface.

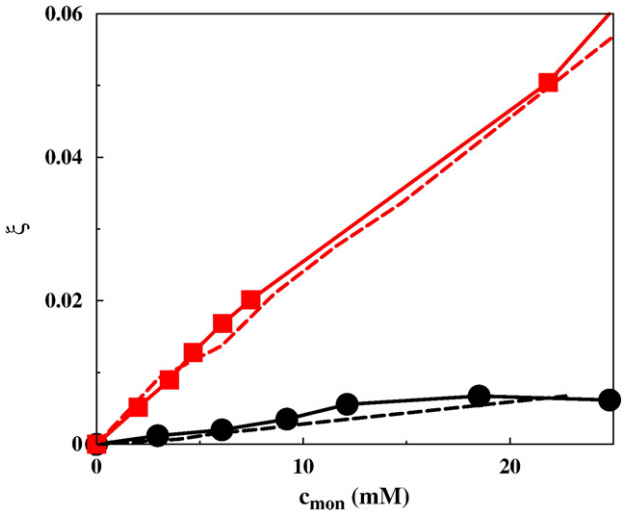

Fig. 8. The adsorbed amount of oligoelectrolyte on C–S–H particles, ξ versus the equilibrium concentration of monomers in the bulk. The adsorbed amount is given as the ratio of adsorbed oligoelectrolyte charge and total amount of Si atoms. pH is approximately 12.5 and the Ca^{2+} concentration is about 20 mM throughout the experiment. Experimental data are shown as black line with circles = dimer and red line with squares = trimer. Simulated adsorption is shown as dashed lines.

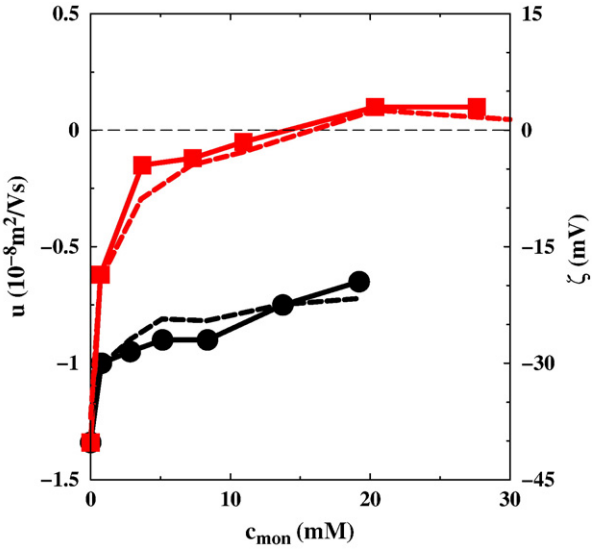

Fig. 9. Measured electrophoretic mobility (u) and simulated electrokinetic potential (ζ) as a function of equilibrium monomer concentration in the bulk. pH is approximately 10 and the Ca^{2+} is about 3 mM. The ionization degree of the C–S–H particles is ≈0.2. The simulated electrokinetic potential is assumed to be located a distance of 6 Å from the surface. Symbols as in Fig. 8.

5. Conclusions

We have demonstrated experimentally that cationic oligoelectrolytes can compete with Ca^{2+} ions as counterions to the C–S–H surface. The adsorption isotherms and electrophoretic mobilities are almost quantitatively reproduced in Monte Carlo simulations of the C–S–H model system, which lends credit to the model. The cohesive forces calculated in simulations of C–S–H in equilibrium with a bulk solution containing both Ca^{2+} and cationic oligoelectrolytes show an interesting behaviour, where the range and magnitude can be tuned with oligomer concentration, polymerization degree, and line charge density. Thus, it seems possible to modulate the ductility and critical strain in cement by addition of cationic polyelectrolytes.

Acknowledgements

The authors would like to acknowledge the industrial ATILH members (http://www.atilh.fr) for a generous grant that allowed them to perform this work. C.L. would like also to acknowledge the support of the CRI from the Université de Bourgogne (https://haydn2005.u-bourgogne.fr/CRI-CCUB/) and of LUNARC from Lund University (http://www.lunarc.lu.se) for access to their computer facilities.

References

[1] X. Cong, R.J. Kirkpatrick, 29Si MAS NMR study of the structure of calcium silicate hydrate, Adv. Cement Based Mater. 3 (1996) 144–156.
[2] G. Constandinides, F.-J. Ulm, The nanogranular nature of C–S–H, J. Mech. Phys. Sol. 55 (2007) 64–90.
[3] S. Gauffinet, E. Finot, E. Lesniewska, A. Nonat, Direct observation of the growth silicate hydrate on alite and silica surfaces by atomic force microscopy, CR Acad. Sci. Paris 327 (1998) 231–236.
[4] H.M. Jennings, A model for the microstructure of calcium silicate hydrate in cement paste, Cement Concr. Res. 30 (2000) 101–116.
[5] A. Nonat, X. Lecoq, The structure, stoichiometry and properties of C–S–H prepared by C3S hydration under controlled solution, in: P. Colombet, A.R. Grimmer, H. Zanni, P. Sozzani (Eds.), Springer-Verlag, BerlinHeidelberg, 1998, pp. 197–207.

[6] T.C. Powers, Structure and physical properties of hardened Portland cement paste, J. Am. Ceram. Soc. 1 (1958) 1–6.
[7] T.C. Powers, T.L. Brownyard, Studies of the physical properties of hardened Portland cement paste, J. Am. Conc. Inst. 1 (1947) 101–132.
[8] G.W. Scherer, Structure and properties of gels, Cement Concr. Res. 29 (1999) 1149–1157.
[9] P.D. Tennis, H.M. Jennings, A model for two types of calcium silicate hydrate in the microstructure of Portland cement pastes, Cement Concr. Res. 30 (1999) 855–863.
[10] I.J. Thomas, H.M. Jennings, A colloidal interpretation of chemical aging of the C–S–H gel and its effects on the properties of cement paste, Cement Concr. Res. 36 (2006) 30–38.
[11] M. Hamlin, H.M. Jennings, Refinements to colloid model of C–S–H in cement: CM-II, Cement Concr. Res. 36 (2008) 257–289.
[12] C. Plassard, E. Lesniewska, I. Pochard, A. Nonat, Investigation of the surface structure and elastic properties of calcium silicate hydrates at the nanoscale, Ultramicroscopy 100 (2004) 331–338.
[13] L.B. Skinner, S.R. Chae, C.J. Benmore, H.R. Wenk, P.J.M. Monteiro, Nanostructure of calcium silicate hydrates in cements, Phys. Rev. Lett. 104 (2010) 195502–195504.
[14] C. Labbez, B. Jönsson, I. Pochard, A. Nonat, B. Cabane, Surface charge density and electrokinetic potential of highly charged minerals: experiments and simulations on calcium silicate hydrate, J. Phys. Chem. B 110 (2006) 9219–9230.
[15] B.V. Derjaguin, L. Landau, Theory of the stability of strongly charged lyophobic sols and of the adhesion of strongly charged particles in solutions of electrolytes, Acta Phys. Chim. URSS 14 (1941) 633–662.
[16] E.J.W. Verwey, J.T.G. Overbeek, Theory of the Stability of Lyophobic Colloids, Elsevier Publishing Company Inc., Amsterdam, 1948.
[17] S. Lesko, E. Lesniewska, A. Nonat, J.-C. Mutin, J.-P. Goudonnet, Investigation by atomic force microscopy of forces at the origin of cement cohesion, Ultramicroscopy 86 (2001) 11–21.
[18] C. Plassard, E. Lesniewska, I. Pochard, A. Nonat, Nanoscale experimental investigation of particle interactions at the origin of the cohesion of cement, Langmuir 21 (2005) 7263–7270.
[19] L. Guldbrand, B. Jönsson, H. Wennerström, P. Linse, Electric double layer forces: a Monte Carlo study, J. Chem. Phys. 80 (1984) 2221–2228.
[20] B. Svensson, B. Jönsson, The interaction between charged aggregates in electrolyte solution: a Monte Carlo simulation study, Chem. Phys. Lett. 108 (1984) 580–584.
[21] R.J.-M. Pellenq, J. Caillot, A. Delville, Electrostatic attraction between two charged surfaces: a (N, V, T) Monte Carlo simulation, J. Phys. Chem. B 101 (1997) 8584–8594.
[22] R.J.-M. Pellenq, A. Delville, H. van Damme, Cohesive and swelling behaviour of charged interfaces: a (N, V, T) Monte Carlo study, in: B. McEnaney, et al., (Eds.), Characterization of Porous Solids IV, The Royal Society of Chemistry, Cambridge, 1997, pp. 596–603.
[23] A. Delville, R. Pellenq, J. Caillot, A Monte Carlo (N, V, T) study of the stability of charged interfaces: a simulation on a hypersphere, J. Chem. Phys. 106 (1997) 7275–7285.
[24] H. van Damme, Colloidal chemo-mechanics of cement hydrates and smectic clays; cohesion vs. swelling, Encyclopedia of Surface and Colloid Science, Marcel Dekker, New York, 2002, pp. 1087–1103.
[25] B. Jönsson, A. Nonat, C. Labbez, B. Cabane, H. Wennerström, Controlling the cohesion of cement paste, Langmuir 21 (2005) 9211–9221.
[26] G.D. Jones, Polyelectrolytes, Technomic, Westerport, CT, 1976.
[27] B. Eriksson, A.M. Härdin, Flocculation in Biotechnology and Separation Systems, Elsevier Science Publishers, Amsterdam, 1987.
[28] K.J. Sasaki, S.L. Burnett, S.D. Christian, E.E. Tucker, J.F. Scamehorn, Polyelectrolyte ultrafiltration of multivalent ions. Removal of copper(2+) by sodium poly (styrenesulfonate), Langmuir 5 (1989) 363–369.
[29] L.C. Gosule, J.A. Schellman, Compact form of DNA induced by spermidine, Nature 259 (1976) 333–335.
[30] R.W. Wilson, V.A. Bloomfield, Polyelectrolyte effects in DNA condensation by polyamines, Biophys. Chem. 11 (1980) 339–343.
[31] A. Nevo, A. deVries, A. Katchalsky, Interaction of basic polyamino acids with the red blood cell. I. Combination of polylysine with single cells, Biochim. Biophys. Acta 17 (1955) 536–547.
[32] T. Åkesson, C. Woodward, B. Jönsson, Electric double layer forces in the presence of polyelectrolytes, J. Chem. Phys. 91 (1989) 2461–2469.
[33] A. Nonat, The structure and stoichiometry of C–S–H, Cement Concr. Res. 34 (2004) 1521–1528.
[34] R.J.-M. Pellenq, A. Kushima, R. Shahsavari, K.J.V. Vliet, M.J. Buehler, S. Yip, F.-J. Ulm, A realistic molecular model of cement hydrates, PNAS 109 (2009) 16102–16107.
[35] D.D. Double, A. Hellawell, S.J. Perry, The hydration of Portland cement, Proc. R. Soc. Lond. A 359 (1978) 435–451.
[36] C. Labbez, B. Jönsson, A new Monte Carlo method for the titration of molecules and minerals, Lect. Notes Comput. Sci. 4699 (2007) 66–72.
[37] C. Labbez, B. Jönsson, Ion–ion correlation and charge reversal at titrating solid interfaces, Langmuir 25 (2009) 7209–7212.
[38] B. Jönsson, H. Wennerström, B. Halle, Ion distributions in lamellar liquid crystals. A comparison between results from Monte Carlo simulations and solutions of the Poisson–Boltzmann equation, J. Phys. Chem. 84 (1980) 2179–2185.
[39] J.P. Valleau, R. Ivkov, G.M. Torrie, Colloid stability: the forces between charged surfaces in an electrolyte, J. Chem. Phys. 95 (1991) 520–532.
[40] D.A. McQuarrie, Statistical Mechanics, Harper Collins, New York, 1976.
[41] D. Frenkel, B. Smit, Understanding Molecular Simulation, Academic Press, San Diego, 1996.
[42] M.N. Rosenbluth, A.W. Rosenbluth, Monte Carlo calculation of the average extension of molecular chains, J. Chem. Phys. 23 (1955) 356–359.
[43] J.I. Siepmann, A method for the direct calculation of chemical potentials for dense chain systems, Mol. Phys. 70 (1990) 1145–1158.
[44] J. Harris, S.A. Rice, A lattice model of a supported monolayer of amphiphile molecules: Monte Carlo simulations, J. Chem. Phys. 88 (1988) 1298–1307.
[45] D. Frenkel, G.C.M. Mooij, B. Smit, Novel scheme to study structural and thermal properties of continuously deformable molecules, J. Phys. Condens. Mater. 4 (1992) 3053–3076.
[46] J.J. DePablo, M. Laso, U. Suter, Estimation of the chemical potential of chain molecules by simulation, J. Chem. Phys. 96 (1992) 2395–2403.
[47] M. Turesson, T. Åkesson, J. Forsman, Interaction between charged surfaces immersed in a polyelectrolyte solution, Langmuir 23 (2007) 9555–9558.
[48] A.K. Kron, The Monte Carlo method in statistical calculations of macromolecules, Polym. Sci. USSR 7 (1965) 1361–1967.
[49] L. Nachbaur, P.-C. Nkinamubanzi, A. Nonat, J.-C. Mutin, Electrokinetic properties which control the coagulation of silicate cement suspensions during early age hydration, J. Colloid Interface Sci. 202 (1998) 261–268.
[50] H. Viallis-Terrisse, A. Nonat, J.-C. Petit, Zeta-potential study of calcium silicate hydrates interacting with alkaline cations, J. Colloid Interface Sci. 244 (2001) 58–65.
[51] L. Sjöström, T. Åkesson, B. Jönsson, Charge reversal in electrical double layers, Ber. Bunsenges. Phys. Chem. 100 (1996) 889–893.